ORGANIC LETTERS

2011
Vol. 13, No. 20
5432–5435

O,O′-Disubstituted *N,N′*-Dihydroxynaphthalenediimides (DHNDI): First Principles Designed Organic Building Blocks for Materials Science

Eric Assen B. Kantchev,*,† Huei Shuan Tan,† Tyler B. Norsten,*,† and Michael B. Sullivan‡

*Institute of Materials Research and Engineering, A*STAR, 3 Research Link, Singapore 117602, and Institute of High Performance Computing, A*STAR, 1 Fusionopolis Way #16-16, The Connexis, Singapore 138632*

kantcheveab@imre.a-star.edu.sg; norstent@imre.a-star.edu.sg

Received July 14, 2011

ABSTRACT

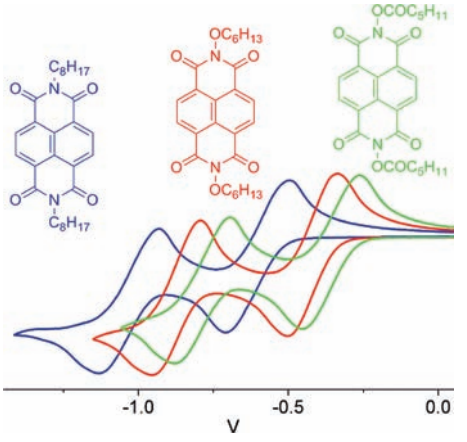

***N,N′*-Disubstituted naphthalenediimides (NDIs), planar, electron-deficient building blocks, play an important role in materials and biological sciences. Naphthalene core substituents control the HOMO and LUMO energies, whereas the *N*-alkyl or aryl substituents affect the solubility, aggregation, and packing propensity in condensed phases. *N,N′*-Dihydroxynaphthalenediimide (DHNDI) allows expanding the chemical diversity by *O*-alkylation, acylation, or sulfonylation; these derivatives also allow fine-tuning of the HOMO/LUMO levels. The synthesis, UV−vis, electrochemical, solid state, and computational prediction of the properties of such derivatives are presented.**

N,N′-Disubstituted naphthalene[1,8:4,5]dicarboxyimides (NDI) are an important class of molecular building blocks employed in polymeric or self-assembled materials used in both material and biological science applications, including chemosensors, n-type organic semiconductors, redox modulators, and fluorescent dyes.[1−3] Substitution in the naphthalene core has a profound effect on the electronic levels related to ionization potential (HOMO) and electron affinity (LUMO).[2] Electron-releasing groups (e.g., alkoxy or amino) raise both the HOMO and LUMO levels to an uneven degree, resulting in a net narrowing of the band gap and a red shift of the absorption maximum into the visible region of the electromagnetic spectrum. On the other hand, the nonsubstituted NDIs or those having electron-deficient

† Institute of Materials Research and Engineering.
‡ Institute of High Performance Computing.

(1) Zhan, X.-W.; Facchetti, A.; Barlow, S.; Marks, T. J.; Ratner, M. A.; Wasiliewski, M. R.; Marder, S. R. *Adv. Mater*. **2011**, *23*, 268–284.
(2) (a) Sakai, N.; Mareda, J.; Vauthey, E.; Matile, S. *Chem. Commun*. **2010**, *46*, 4225–4237. (b) Bhosale, R.; Míšek, J.; Sakai, N.; Matile, S. *Chem. Soc. Rev*. **2010**, *39*, 138–149.
(3) Bhosale, S. V.; Jani, C. H.; Langford, S. J. *Chem. Soc. Rev*. **2008**, *37*, 331–342.

10.1021/ol201906z
Published on Web 09/22/2011

substituents (fluoro- or cyano-) behave as excellent electron acceptors as a consequence of lowering of both the HOMO and LUMO levels. The *N*-substituents play a role in modulating the solubility and self-assembly propensity of these highly aggregation-prone, planar aromatic compounds.[4] In condensed phases, the macroscopic properties of the material are affected by numerous cooperative weak interactions among these side chains.[5] As a consequence, such effects can be strong yet nonlinear and unpredictable. For instance, whereas *N*,*N*′-dihexyl-NDI exhibits modest electron mobility in vapor-deposited thin films (0.7 $cm^2\ V^{-1}\ s^{-1}$), the corresponding *N*,*N*′-dicyclohexyl derivative shows one of the highest mobilities (6.2 $cm^2\ V^{-1}\ s^{-1}$) recorded for a small molecule n-type semiconductor.[6] This has been rationalized by the latter being highly organized in the solid state whereas the former is disordered as a result of unfavorable side chain packing as demonstrated by single crystal and X-ray diffraction analysis. Synthetically, NDIs are only accessible from primary alkyl and aryl amines.[3] This limits both the chemical diversity and, as we will show, the electron affinities attainable in the NDI scaffold.

The nitrogen atom in hydroxylamine is more electron-deficient than in ammonia, reflected in the large pK_a difference between NH_3OH^+ (pK_a = 5.94) and NH_4^+ (pK_a = 9.23). Hence, we reasoned that incorporation of an *O*-substituted hydroxylimide instead of an imide would lead not only to a lowering of the LUMO but also opening of a route to hitherto unexplored NDI derivatives by *O*-alkylation, *O*-acylation, or *O*-sulfonylation (Figure 1). The latter two types of derivatives are synthetically inaccessible for NDIs. Notably, *N*,*N*′-dimethoxyNDI was shown as far back as 1992 to have lower first ($E_{1/2}{}^1{}_{red}$, 0.39 vs 0.54) and second ($E_{1/2}{}^2{}_{red}$, 0.86 vs 0.98) reduction potentials vs SCE compared to the unsubstituted NDI (**1**).[7] Computational modeling of the unsubstituted DHNDI (**2**) (M06[8]/DGTZVP[9] level of theory) further confirmed

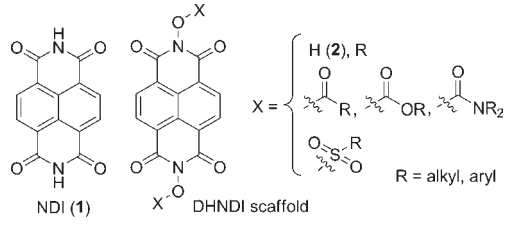

Figure 1. Potential chemical diversity of *O*-functionalized derivatives of *N*,*N*′-dihydroxynaphthalenediimide (DHNDI).

Table 1. DFT (M06/DGTZVP) Characterization of *O*-Functionalized DHNDI Derivatives[a]

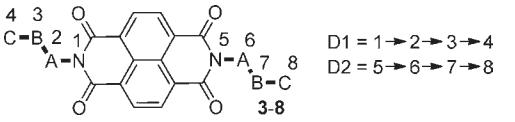

	A	B	C	D1, deg	D2, deg	Q_{zz}, B	ΔG, kcal mol^{-1}
3a	CH_2	CH_2	Me	180.0	180.0	6.1	0.00[b]
3b				179.8	62.6	5.8	0.55
3c				−62.4	62.4	5.3	1.93
4a	O	CH_2	Me	180.0	180.0	5.2	0.00[b]
4b				178.7	67.3	4.7	1.51
4c				−68.7	68.7	4.0	3.89
5a	O	C=O	Me	180.0	180.0	−10.2	0.00[b]
5b				180.0	0.0	10.8	6.44
5c				0.0	0.0	32.0	13.0
6a	O	C=O	CF_3	178.4	−178.4	12.0	0.00[b]
6b				180.0	0.3	16.8	6.33
6c				0.0	0.0	19.0	13.4
7a	O	C=O	NMe_2	179.5	179.3	−18.2	0.00[b]
7b				179.8	35.0	2.3	12.1
7c				35.6	35.6	18.5	24.0
8a	O	SO_2	Me	115.5	−115.6	0.2	0.00[b]
8b				115.8	115.8	0.4	0.17

[a] An *N*,*N*′-dialkyl NDI derivative is shown for comparison [b] Chosen as the reference structure.

that *N*-hydroxylation leads to a substantial decrease of LUMO energy relative to **1** (−3.97 vs −3.69 eV).

Functionalization at the hydroxy group is expected to affect not only the frontier orbital energies but also the side-chain conformation. We explored the conformational preferences and the frontier orbitals of various *O*,*O*′-disubstituted DHNDI derivatives (**4-8**) at M06/DGTZVP level of theory in gas phase (Table 1) and in implicit CH_2Cl_2 (SMD;[10] see Supporting Information (SI)). The properties of *N*,*N*′-dipropyl NDI (**3**) were also evaluated for comparison. The side chain in **3** has two potential energy minima at the $N-CH_2-CH_2-CH_3$ dihedral angle (D2) values of ∼60° and 180°. Therefore, taking into account the symmetry of (DH)NDI, **3**, side chain conformations (**3a**−**c**) are possible. The 180/180 conformation (**3a**) (ΔG = 0.00 kcal mol^{-1}) was the most stable, followed by 180/60 (**3b**) (ΔG = 0.55 kcal mol^{-1}) and 60/60 (ΔG = 1.93 kcal mol^{-1}). The D2 angle for the *N*,*N*′-diethoxy derivative **4** was similar. Energetically, however, the conformations are considerably further apart (ΔG = 0.00, 1.51, and 3.89 kcal mol^{-1} for 180/180, 180/70, and 70/70, respectively). This implies that the percentage of the most

(4) (a) Molla, M. R.; Ghosh, S. *Chem. Mater.* **2011**, *23*, 95–105. (b) Anderson, T. W.; Sanders, J. K. M.; Pantoş, G. D. *Org. Biomol. Chem.* **2010**, *8*, 4274–4280. (c) Shao, H.; Parquette, J. R. *Chem. Commun.* **2010**, *46*, 4285–4287.

(5) (a) Bell, T. D. M.; Bhosale, S. V.; Forsyth, C. M.; Hayne, D.; Ghiggino, K. P.; Hutchinson, J. A.; Jani, C. H.; Langford, S. J.; Lee, M. A.-P.; Woodward, C. P. *Chem. Commun.* **2010**, *46*, 4881–4883. (b) Nakatsuji, S.; Aoki, K.; Akutsu, H.; Yamada, J.; Kojima, T.; Nishida, J.; Yamashita, Y. *Bull. Chem. Soc. Jpn.* **2010**, *83*, 1079–1085.

(6) Shukla, D.; Nelson, S. F.; Freeman, D. C.; Rajeswaran, M.; Ahearn, W. G.; Meyer, D. M.; Carey, J. T. *Chem. Mater.* **2008**, *20*, 7486–7491.

(7) Zhong, C.-J.; Kwan, W.-S. V.; Miller, L. L. *Chem. Mater.* **1992**, *4*, 1423–1428.

(8) Zhao, Y.; Truhlar, D. *Theor. Chem. Acc.* **2008**, *120*, 215–241.

(9) Godbout, N.; Salahub, D. R.; Andzelm, J.; Wimmer, E. *Can. J. Chem.* **1992**, *70*, 560–571.

(10) Marenich, A. V.; Cramer, C. J.; Truhlar, D. *J. Phys. Chem. B* **2009**, *113*, 6378–6396.

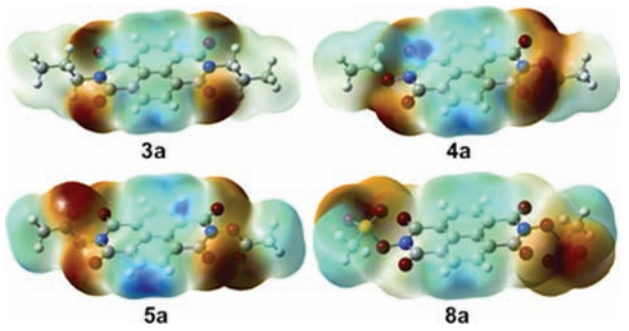

Figure 2. Electrostatic potential-mapped total electronic densities (blue = positive, red = negative) contour maps for minimum energy conformations of selected DHNDI derivatives.

stable 180/180 conformation is significantly increased for the alkoxy vs the alkyl substituent, possibly having a beneficial effect on crystal packing and $\pi-\pi$-stacking in the condensed state. The *O*,*O*′-dicarbonyl derivatives all show two minimum energy D2 angles at 180° and 0°. Even small carbonyl substituents favor a 180° conformation by a large energetic margin: CH_3 (**5a**–**c**), ΔG = 0.00, 6.44, and 13.0 kcal mol^{-1} for 180/180, 180/0, and 0/0, respectively, and CF_3 (**6a**–**c**) ΔG = 0.00, 6.33, and 13.4 kcal mol^{-1}, respectively. In contrast, the mesolate derivative has only one minimum energy D2 angle of ~120°, resulting in two conformations (**8a**, **b**) with almost equal energy. The energies in implicit solvent (CH_2Cl_2), while slighly smaller, follow the same trends. Also, the general decrease of the quadrupole moment (Table 1) (with exception of **6**) relative to *N*,*N*′-dipropyl NDI **3** for the minimum conformations despite the more electron-deficient naphthalene rings (Figure 2) is noteworthy.

The published synthesis of DHNDI (**2**) by reaction of dianhydride **9** with hydroxylamine in aqueous medium affords **2** as a hydrate in low yield after recrystallization.[7] We developed a new, large scale synthesis in DMF, which allows pure **2** to be isolated water-free after simple filtration in 89% yield (Scheme 1). Acylation of **2** with *n*-hexanoyl (**10**, 74%) or the bulky pivaloyl (**11**, 77%) chlorides was straightforward, and Mitsunobu alkylation (1-hexanol) was fast and clean to give **12** in 79% yield.

Scheme 1. Synthesis of *O*-Substituted DHNDI Derivatives

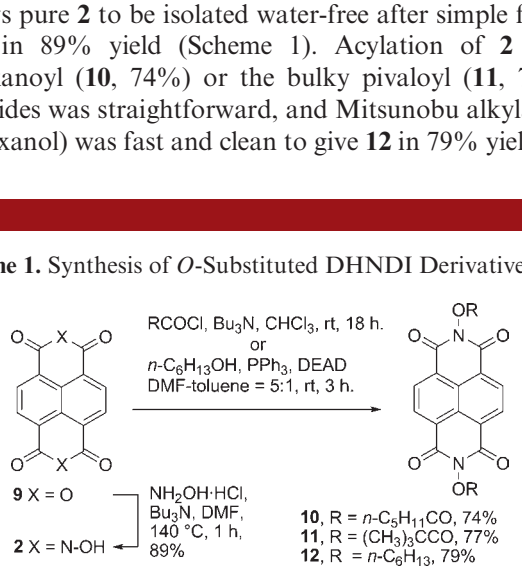

The UV spectra of **10**–**12** display similar characteristic electronic S_0-S_1 absorption bands (Figure 3a). The known *N*,*N*′-dioctyl NDI[11] (**13**) displays the longest wavelength absorption, and as expected from our computations, the introduction of the *O*-alkyl group (**12**) and the most electron-withdrawing *O*-acyl groups (**10**–**11**) results in a systematic (*O*-acyl > *O*-alkyl > *N*-alkyl) hypsochromic shift of the S_0-S_1 UV absorption transitions (Table 2).

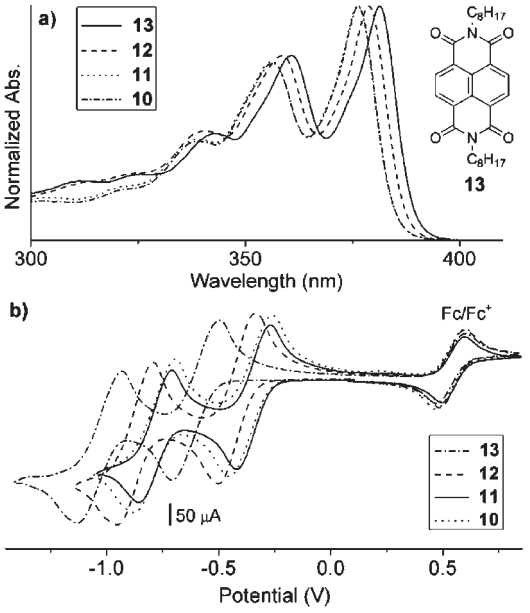

Figure 3. (a) UV spectra of NDI **13** and DHNDIs **10**-**12** in $CHCl_3$ and (b) CVof NDI **13** and DHNDIs **10**–**12** in 0.1 M $TBAPF_6$ in CH_2Cl_2 at sweep rate of 50 mV s^{-1}.

The cyclic voltammograms of compounds **10**–**13** exhibit two reversible reductions that are separated by about 450 mV (Figure 3b). All DHNDI derivatives display anodically shifted reduction waves compared to *N*,*N*′-dialkyl NDI **13**. The shift was more pronounced for *O*-acyl derivatives (**10**–**11**) than the *O*-alkyl (**12**). The LUMO energies relative to the vacuum were obtained by subtraction

Table 2. Optical and Electrochemical Properties of NDI and DHNDI Compounds

	λ_{max}[a] (nm)	E_g^{opt}[b] (eV)	$E_{1/2}{}^1{}_{red}$[c] (V)	$E_{1/2}{}^2{}_{red}$[c] (V)	LUMO[d,f] (eV)	HOMO[e,f] (eV)
10	376	3.19	−0.88	−1.34	−4.22 (−3.42)	−7.41 (−7.46)
11	376	3.19	−0.87	−1.32	−4.23	−7.42
12	379	3.16	−0.96	−1.41	−4.14 (−3.32)	−7.30 (−7.35)
13	382	3.14	−1.14	−1.57	−3.96 (−3.18)	−7.10 (−7.20)

[a] Solution absorption spectra 3×10^{-5} M DCM. [b] Optical energy gap estimated from the UV absorption edge. [c] CV measurements in DCM solution vs Fc/Fc^+. [d] Estimated from LUMO = $-5.1 - E_{1/2}{}^1{}_{red}$. [e] Estimated from HOMO = LUMO − E_g^{opt}. [f] Theoretical (SMD/M06/DGTZVP in CH_2Cl_2) values for structures **5a**, **4a**, and **3a** as analogs of **10** and **11**, **12**, and **13**, respectively, are shown in brackets.

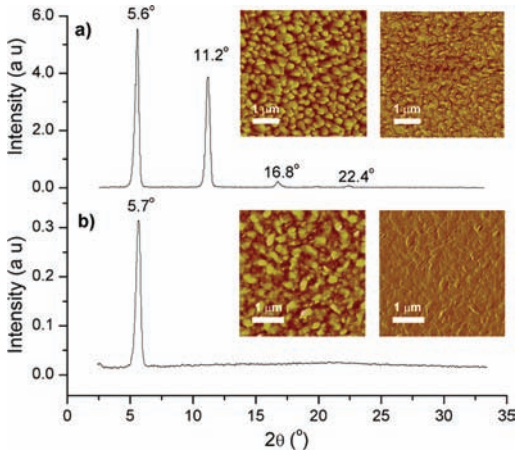

Figure 4. XRD intensity graphs and AFM height (left inset) and phase (right inset) images of vacuum deposited films of **11** (a) and **12** (b) on OTS-modifed Si/SiO_2 substrates.

of −5.1 eV for Fc/Fc^+ from the first redox potentials.[12] Substitution of DHNDIs for the prototypical NDIs results in a stronger electron affinity of the napthalene core and a lowering (by ∼0.2−0.3 eV) of the LUMO level (Table 2). The frontier orbital energies for the lowest energy conformer calculated at the SMD/M06/DGTZVP level of theory in CH_2Cl_2 were systematically shifted by $+0.80 \pm 0.02$ eV for the LUMO and −0.05 to −0.10 eV for the HOMO, the trends confirming the validity of our computational design. Usually, the FMO energies of NDI derivatives are lowered by core substitution by an electron-deficient substituent, most often fluoro or cyano.[2,12] The alternative strategy of side-chain modification to the same end is often discounted because of the presence of a node on the nitrogen atom in NDIs.[13] However, in this work we demonstrate that the latter is a viable strategy, even though the changes in FMO energies are less drastic. Notably, the general shapes of the FMOs are preserved going from NDI to DHNDI (see SI). A similar effect has recently been observed for NDI di-*N*-substituted with 3,5-bis(trifluoromethyl)aniline vs aniline[14] and *N*-acyl vs *N*-alkyl dithieno[3,2-*b*:2′,3′-*d*]pyrroles demonstrating the generality of this approach to LUMO lowering/fine-tuning.[15]

The atomic force microscopic (AFM) image of a thin film of **11** shows a densely packed polycrystalline film with an average feature size of ∼100 nm (Figure 4a inset). The X-ray diffractogram (XRD) of this film showed strong and narrow peaks up to the fourth order (Figure 4a). The close correspondence between the molecular length of **11** (16.0 Å, obtained from DFT) and interlayer regular *d*-spacing of 15.8 Å in the XRD suggests that thin films of **11** grow with the long axis of the molecule oriented out of the substrate plane. In contrast, the AFM image of the thin film of **12** shows a more loosely packed polycrystalline film with a significantly larger grain size (∼500 nm) (Figure 4b inset). However, the XRD of the thin film of **12** shows only one diffraction peak (Figure 4b). Thin films of **12** could also be prepared by spin coating $CHCl_3$ solutions onto OTS modified Si/SiO_2 substrates. For these films, XRD was virtually identical (see SI) while AFM showed substantially larger grain sizes (∼1 μm).

In conclusion, we have demonstrated that computationally designed *O*,*O*′-dialkyl or acyl *N*,*N*′-dihydroxynaphthalene-[1,8:4,5]diimides have stronger electron affinities than the widely used *N*,*N*′-dialkylnaphthalene[1,8:4,5]diimides. Further studies on the application of these novel building blocks for the design of organic electronic materials are in progress.[16]

Acknowledgment. This work was funded by the Institute of Materials Research and Engineering (IMRE) and Institute of High Performance Computing (IHPC), Science and Engineering Research Council (SERC), Agency for Science, Technologies and Research (A*STAR). We thank A*STAR Computational Resource Centre (A*CRC) for generous grants of CPU time on the Fuji Linux cluster.

Supporting Information Available. Expanded Table 1; computational methodology, additional references and results for **1**−**8** and **11**; synthetic procedures and characterization data for **2**, **10**−**12**; OTFT device characterization for **11** and **12**; general procedures for CV, UV spectroscopy, AFM and XRD of solution cast film studies. This material is available free of charge via the Internet at http://pubs.acs.org.

(11) Gryko, D. T.; Rogacki, M. K.; Klajn, J.; Galezowski, M.; Stepien, D. K.; Cyranski, M. K. *Org. Lett.* **2010**, *12*, 2020–2023.
(12) Misek, J.; Jentzsch, A. V.; Sakurai, S.; Emery, D.; Mareda, J.; Matile, S. *Angew. Chem., Int. Ed.* **2010**, *49*, 7680–7683.
(13) (a) Huang, C.; Barlow, S.; Marder, S. R. *J. Org. Chem.* **2011**, *76*, 2386–2407.
(14) Evenson, S, J.; Rasmussen, S, E. *Org. Lett.* **2010**, *12*, 4054–4057.
(15) Jung, Y.-O.; Baeg, K.-J.; Kim, D.-Y.; Someya, T.; Park, S.-Y. *Synth. Met.* **2009**, *159*, 2117–2121.
(16) The thin film transistor properties of **11**−**12** were evaluated as a channel semiconductor employing a bottom-gate, top-contact OTFT configuration but failed to show any electron mobility (see SI).